Monograph:
Lui, J., Billings, S.A., Zhu, Z.Q. et al. (2001) Enhanced Frequency Analysis Using Wavelets. Research Report. ACSE Research Report 790 . Department of Automatic Control and Systems Engineering

Enhanced Frequency Analysis using Wavelets

J. Liu[a], S. A. Billings[a], Z. Q. Zhu[b] and J. Shen[b]

(a) Department of Automatic Control & Systems Engineering,
The University of Sheffield, Mappin Street,
Sheffield S1 3JD, England
(b) Department of Electronic & Electrical Engineering,
The University of Sheffield, Mappin Street,
Sheffield S1 3JD, England

Research Report No. 790
May 2001

Enhanced Frequency Analysis using Wavelets

J. Liu[a], S. A. Billings[a], Z. Q. Zhu[b] and J. Shen[b]

(a) Department of Automatic Control & Systems Engineering,

The University of Sheffield, Mappin Street,

Sheffield S1 3JD, England

(b) Department of Electronic & Electrical Engineering,

The University of Sheffield, Mappin Street,

Sheffield S1 3JD, England

Abstract: An enhanced frequency analysis method is introduced using a phase shift wavelet representation to analyze individual frequency components and to reveal features of a given signal. The frequency representation provides details at each time location without the loss caused by local orthogonality between the wavelet basis functions and the given signal which occurs when a normal wavelet decomposition is employed. Movement of the local orthogonality locations, corresponding to the phase shift of the wavelet basis functions, are studied and it is shown that these movements are important and can be used to reveal features of the signal in the frequency domain, such as continuities, smoothness, and trends. Several examples are presented to illustrate the method and an application to a permanent magnet synchronous drive system is provided to demonstrate the approach.

1 Introduction

Wavelets have been extensively studied and applied by scientists and engineers from many different backgrounds. Wavelet theory is an interesting mathematical subject which has links to many other areas including functional analysis, approximation theory and numerical analysis. Wavelets are widely applied in many fields including signal processing, image processing, communications, geographical data processing and financial analysis.

There are many research studies on basic wavelet theory, especially related to operator theory, approximation theory, function spaces (L^2, L^p, Besov, Sobolev and Holder) and orthogonal, orthonormal and biorthogonal bases. Daubechies [1][2] provided a good mathematical introduction to wavelets including a list of wavelet basis functions, while Chui [3] gave a description from the point of view of approximation.

Parallel to contributions in the area of wavelet theory, many studies have focused on bridging the gap between basic theory and applications. Juditsky et al [4] summarized the important properties of wavelets for approximation in Besov space, including norm evaluation with orthonormal wavelet decompositions, sparse singularities with wavelet decomposition, and the advantages of spline-wavelets. Pati and Krishnaprasad [5] formed a representation of a class of feedforward neural networks in terms of discrete affine wavelet transforms, and Zhang et al [6] introduced another wavelet network for approximating arbitrary nonlinear functions.

The computational aspects of wavelets is very important for achieving an acceptable accuracy, especially in multidimensional situations. Juditsky et al [4] noted that wavelet-based estimation algorithms are the only class of algorithm for which a complete analysis is available today, both for approximation and estimation. In Besov space, norms are easily evaluated using wavelet decompositions. In 1997, Zhang [7] proposed algorithms for the construction of a wavelet network to improve the computational efficiency so that problems which involve large dimensions can be better handled.

The advanced application of wavelets can generally be divided into two aspects, approximation and representation. Wavelet approximations are used in many fields. Stone [8] combined Fourier and wavelet packet transforms to exploit the advantages of each technique. Multiresolution analysis was introduced in Meyer [9] and Mallat [10] and further developed by Daubechies, this was an important development and made wavelet approximations much more powerful. This approach has been used not only to construct wavelets, but also for algorithm development. Coca and Billings [11] used a nonorthogonal multiresolution wavelet decomposition to smooth and then to differentiate observed noisy signals, and to provide the information needed to approximate a continuous-time description of the system of interest as a set of nonlinear differential equations.

Wavelet representations have also been widely applied in filtering and filter bank design. Up to July 1999 over 200 papers had appeared in IEEE Transaction on Signal Processing related to wavelets. Over 25% of these discussed filters and filter banks based on orthogonal, orthonormal or biorthogonal wavelet decompositions, including a special issue on the theory and application of filter banks and wavelet transformations. Nowak et al [12] introduced two new structures for nonlinear signal processing, which are based on a two-step decomposition consisting of a linear orthogonal signal expansion followed by a scalar polynomial transformation of the resulting signal coefficients. Xia et al [13] discussed the design of optimal multifilter banks and optimum time-frequency resolution multiwavelets with different objective functions, and presented the symmetric extension transform which is related to multifilter banks with symmetric properties. Evangelista et al [14] presented a perfect-reconstruction filter bank based on classical sampled filter banks by means of frequency transformations. Miller et al [15] proposed a method for selecting pre/post filter coefficients to adaptively initialize multiwavelet decompositions of 1-D data sets. Jiang [16] gave several parametric expressions for orthogonal causal FIR multifilter banks, and based on parametric expressions for orthogonal multiwavelet banks, orthonormal multiwavelet pairs with good time-frequency resolution were constructed. Wavelet representations are widely used in image processing, image coding, image compression, de-noising, object recognition, object detection and recovery, tomographic reconstruction and seismic reflection identification.

In this paper, a new approach to enhance frequency analysis using wavelets is introduced. Any given signal can be decomposed into individual frequency components. The advantage of a wavelet decomposition is that this provides more accurate time locations than if a windowed Fourier Transformation is used. The question addressed here is how faithful the frequency components can be represented by a wavelet decomposition at each location. Because the signal can be orthogonal with a wavelet basis function at certain locations, this

can cause information loss in the wavelet representation at these locations. Initially, a phase shift wavelet decomposition is derived by introducing a phase shift parameter. The relationship between the features of the signal and the movement of the local orthogonalities corresponding to phase shifts is then studied. Several examples are used to illustrate the new method and an application to a permanent magnet synchronous drive system is shown.

This paper is organized as follows. In section 2, the main features of wavelet representations are summarized. In section 3, the new method which involves shifting the phase of the wavelet basis functions to analyze the frequency components of a wavelet decomposition for a given signal is introduced. In section 4, three examples are analyzed using the new phase shift method. In section 5, a real application to a permanent magnet synchronous motor is analyzed, and an improvement in the motor control strategy is achieved. Conclusions are given in the last section.

2 Wavelet Representations

A signal $S(t)$ can be expanded in the form

$$S(t) = \sum_{j,k} < S(t), \psi_{j,k}(t) > \psi_{j,k}(t) \qquad (1)$$

where $< \cdot >$ is the inner product; and $\psi_{j,k}(t)$ is the wavelet basis function generated from a mother wavelet.

Many function spaces have been explored to investigate admissible functions for mother wavelets. The choice of a mother wavelet depends on the given signal since each class of functions has certain features which can be matched with certain signals. For example, the Harr wavelet is often used to approximate piecewise-constant functions because this produces a better convergence rate than any other class of functions.

A mother wavelet function is usually denoted as $\Psi_{a,b}(x) = |a|^{1/2} \Psi(\frac{x-b}{a})$, where a is the dilation or scale parameter and b is the location. To approximate a signal, a wavelet framework has to be built and this will include selecting an admissible function as the mother wavelet and determining the parameters a and b. Based on this framework, a wavelet representation can be generated.

The study of wavelet frameworks will influence the approximation strategy in various function spaces. For example, Besov spaces, which consist of a wide family of function classes, are suitable for analyzing both uniformly smooth functions and locally spiky and jumpy functions, but it is not so easy to determine an optimal approximation. However, wavelets provide a good solution for approximation in Besov spaces. Wavelets are as good as splines, but are much easier to construct, and the norms are easily evaluated.

For different selections of a and b in $\Psi_{a,b}(x)$, there will be a different framework, as well as a different wavelet representation. Ideally, a wavelet decomposition with different frameworks can reach the same approximating accuracy in reconstruction, however, the features of the signal revealed by the wavelet

representation and the computing efficiency can be quite different. Therefore, a proper selection of a and b is important for signal analysis using a wavelet representation. Usually, the parameters a and b are selected as $a=\frac{1}{2^j}$, and $b=\frac{k}{2^j}$, $j,k \in Z$.

The combination of all the frequency components generated from a wavelet decomposition can approximate the signal with a desired accuracy. However, whether the wavelet representation faithfully represents the signal at each time location for all the frequency components can be a problem.

3. A Phase Shift Wavelet Frequency Description

A given signal can be decomposed into different frequency components using a wavelet decomposition, and each frequency component can then be studied individually at any location. However, there are some special situations, which arise when the signal is orthogonal to some wavelet basis functions at certain locations. In this case, the energies at the corresponding frequency components, at these locations, can fail to be revealed. Such a situation may not affect the approximation accuracy at the location, for it can be compensated by neighboring frequency components. But when the aim is to study every detail of a frequency component at all the locations in order to form an expression, or to get an exact frequency distribution of the signal, then it is important to overcome this failure of energy detection at certain locations. This problem is caused by local orthogonality between the signal and the wavelet basis function.

3.1 Avoiding Problems caused by Local Orthogonality in Frequency Component Analysis

In order to avoid the loss in the wavelet representation of individual frequency components caused by local orthogonalities between the signal and wavelet basis functions, it is necessary to study how to remove local orthogonalities at certain locations.

Suppose $S(t)$ is a given signal, that can be represented by a wavelet expansion as in equation (1), where the mother function $\psi(t)$ has been selected from the many kinds of function spaces to match the characteristics of the signal $S(t)$, and the dilations are $\psi_{j,k}(t) = 2^{j/2}\psi(2^j t - k)$. Ideally, the number of frequency components should be infinite, but in practice, this is impossible. Suppose $j = N_1, N_1+1, ..., N_2$, $N_1, N_2 \in Z$, and the signal $S(t)$ is approximately represented as

$$S_w(t) = \sum_{j=N_1}^{N_2} \sum_{k=0}^{k_j} \langle S(t), \psi_{j,k}(t) \rangle \psi_{j,k}(t) \qquad (2)$$

The local orthogonality condition states that for a small $\varepsilon > 0$, there are $j', k' \in Z$, such that in the support intervals $[2^{-j'}k', 2^{-j'}(k'+1)]$, the signal satisfies the following

$$\int_{2^{-j'}k'}^{2^{-j'}(k'+1)} |S(t)| dt \neq 0 \qquad (3a)$$

$$\left\langle S(t), \psi_{j',k'}(t) \right\rangle = 0 \tag{3b}$$

$$\left\langle S(t), \psi_{j',k'}(t \pm \varepsilon) \right\rangle \neq 0 \tag{3c}$$

where $t \in [2^{-j'}k', 2^{-j'}(k'+1)]$.

Since a wavelet framework is determined by three key factors, the mother wavelet, the dilation parameter a, and the location parameter b, any modification of these factors can change the framework to give a new wavelet representation in which the locations of local orthogonalities would be completely changed. It is not necessary to modify all these three factors to remove a local orthogonality at a certain location, only the simplest factor, the location parameter b is enough. Therefore a small parameter will be introduced to adjust the phase of the wavelet basis functions.

By introducing a phase shift parameter p, the wavelet representation of $S(t)$ becomes

$$S_{wp}(t) = \sum_{j=N_1}^{N_2} \sum_{k=0}^{k_j} < S(t), \psi_{j,k}(t-p) > \psi_{j,k}(t-p) \tag{4}$$

and $\int_{2^{-j'}k'}^{2^{-j'}(k'+1)} |S(t)| dt \neq 0, < S(t), \psi_{j',k'}(t-p) > \neq 0 \; (t \in [2^{-j'}k', 2^{-j'}(k'+1)])$.

The phase changes the location slightly, and the signal $S(t)$ is therefore no longer orthogonal with the wavelet basis function $\psi_{j',k}(t-p)$ at $k = k'$. However, it is possible to induce local orthogonalities between $S(t)$ and $\psi_{j',k}(t-p)$ at other locations. This problem can be resolved by generalizing this method further.

Introduce a set of phase shift parameters, $p = [p_m; m = 0,1,2,..., r]$, so that $S(t)$ can now be represented as

$$S_{w1}(t) = \sum_{j=N_1}^{N_2} \sum_{k=0}^{k_j} < S(t), \psi_{j,k}(t-p_1) > \psi_{j,k}(t-p_1) \tag{5a}$$

$$S_{w2}(t) = \sum_{j=N_1}^{N_2} \sum_{k=0}^{k_j} < S(t), \psi_{j,k}(t-p_2) > \psi_{j,k}(t-p_2) \tag{5b}$$

...

$$S_{wr}(t) = \sum_{j=N_1}^{N_2} \sum_{k=0}^{k_j} < S(t), \psi_{j,k}(t-p_r) > \psi_{j,k}(t-p_r) \tag{5r}$$

The expressions in (5) should reach the same approximation accuracy when reconstructed. However, the frequency components in (5) will usually be different at any given location. Consider only one frequency component, $j = j'$, which is denoted as $S_w^{j'}$, then

$$S_{w1}^{j'}(t) = \sum_{k=1}^{k_j} < S(t), \psi_{j',k}(t-p_1) > \psi_{j',k}(t-p_1) \tag{6a}$$

$$S_{w2}^{j'}(t) = \sum_{k=1}^{k_j} < S(t), \psi_{j',k}(t - p_2) > \psi_{j',k}(t - p_2) \qquad (6b)$$

...

$$S_{wr}^{j'}(t) = \sum_{k=1}^{k_j} < S(t), \psi_{j',k}(t - p_r) > \psi_{j',k}(t - p_r) \qquad (6r)$$

The signal $S(t)$ can not be orthogonal simultaneously, at any particular location with all the wavelet basis functions $\psi_{j',k}(t - p_i)$, $i = 1,2,...,r$. $\{S_{wi}^{j'}(t)\}$, $i = 1,2,...,r$ can therefore be regarded as a complete wavelet representation at the frequency component $j = j'$. Therefore an accurate distribution of energy in $S(t)$ at the frequency component $j = j'$ can be obtained by synthesizing all the representations of frequency component $j = j'$ in (6) without a loss caused by local orthogonality.

For all j, a complete wavelet frequency component description can therefore be obtained which could be important in situations where an enhanced frequency analysis is required.

3.2 Frequency Component Analysis Using Local Orthogonality

In the previous subsection, a method was suggested to overcome problems caused by local orthogonality at frequency components. While this does not affect the approximation accuracy it can result in a failure to reveal the exact energy distribution in the wavelet representation. When a small phase shift is added to the wavelet basis function, the local orthogonalities will be destroyed but other local orthogonalities may be generated. If the phase shift is doubled, the local orthogonalities will be changed again. Therefore, the local orthogonalities will be moved rather than reduced. These movements are closely connected with the features of the signal. Sometimes, the trajectory of the local orthogonality corresponding to the variation of the phase shift can describe the features of the signal very well, especially when the signal locally is approximately equal to a special function, such as a piecewise-constant, a monotone continuous function, or other special functions in the time-frequency domain.

Let $\{p_m\}, m = 0,1,2,...,r$, be a set of phase shift values. Where $p_0 = 0$, $p_r = 2^{-j'}$, $p_1 = p_2 - p_1 = p_3 - p_2 = ... = p_r - p_{r-1}$. Assume that corresponding to each p_m, $m = 0,1,2,...,r$, there is a wavelet decomposition of the frequency components at $j = j'$ as described in (6). Let $C_{k,m}$ $(k = 1,2,...,k_{j'}; m = 0,1,2,...,r)$ denote the inner products $< S(t), \psi_{j',k}(t - p_m) >$ for the frequency component $j = j'$. Then since $p_r = 2^{-j'}$,

$$\begin{aligned} C_{k,r} &= < S(t), \psi_{j',k}(t - p_r) > \\ &= < S(t), \psi[2^{j'}(t - 2^{-j'}) - k] > \\ &= < S(t), \psi[2^{j'}t - (k+1)] > \end{aligned}$$

$$= C_{k+1.0}$$

This implies that only p_m ($m = 0,1,2,...,r-1$) is necessary.

Using all of the phase shift values $p_m, m = 0,1,2,...,r-1$, and collecting the inner products $< S(t), \psi_{j',k}(t - p_m) >$ at all the locations, a matrix, formed from a location-phase section, can be obtained as follows:

$$\begin{bmatrix} C_{1.0} & C_{2.0} & \cdots & C_{k_{j'}.0} \\ C_{1,1} & C_{2.1} & \cdots & C_{k_{j'}.1} \\ \cdots & \cdots & \cdots & \cdots \\ C_{1,r-1} & C_{2.r-1} & \cdots & C_{k_{j'}.r-1} \end{bmatrix} \tag{7}$$

This is the coefficient matrix of the wavelet representation of the component $j = j'$. Each row in the matrix (7) belongs to a wavelet decomposition of the signal $S(t)$, and the column vectors describe how $C_{k,0}$, $k \in \{1,2,...,k_{j'-1}\}$ becomes $C_{k+1,0}$, $k \in \{1,2,...,k_{j'-1}\}$. However, $C_{k,m}(m = 1,2,...,r-1)$ are not limited to the interval $[\min(C_{k,0}, C_{k+1.0}), \max(C_{k,0}, C_{k+1.0})]$, $k \in \{1,2,...,k_{j'-1}\}$. All the $C_{k.m} = 0, k \in \{1,2,...,k_{j'-1}\}$, and $m \in \{1,2,...,r-1\}$, which are caused by local orthogonality can be collected in matrix (7).

When the phase is shifted by a certain value, a local orthogonality will be removed but a new orthogonality may be created. If the distance between the location of the newly created local orthogonality and the location of the previous local orthogonality is not beyond a defined value, the newly created local orthogonality can be regarded as being moved from the location of the previous local orthogonality.

A method was introduced to search for the movement of the local orthogonanlity. This starts from each location and searches for the movement of the orthogonal location corresponding to the phase shift around a given radius. Different search radii can be adopted during the search process, but a large search radius may fail to find the arrival and departure locations while a small radius may fail to find the movements.

The location, to where the local orthogonality moves, is defined as an arrival point. The farthest location, from where the local orthogonality moves to the arrival point, is defined as the departure point.

The departure points and the arrival points often reveal that the signal, in the time-frequency domain, is not smooth at these locations, or smooth but orthogonal with the wavelet basis function at this frequency component.

4 Simulated Examples

In this section, four simulated examples are presented to illustrate the ideas which were introduced in the previous sections.

4.1 Example 1

This example was chosen to demonstrate the phase shift wavelet decomposition method for frequency

component analysis. The data in Figure 1 (a) was produced by simulating the Duffing equation

$$y'' + 0.1y' + y^3 = 11\cos t \tag{8}$$

Figure 1 (b) shows the normal wavelet frequency component representation for $j = -4$. This frequency component $j = -4$ shows that there are 12 sharp peaks and troughs. However, a comparison with the original signal shows that there should be 19 or 20 sharp peaks and troughs, clearly therefore some of the sharp peaks have not been detected. A clearer frequency component representation for $j = -4$ is obtained by using the phase shift wavelet decomposition, and this is shown in Figure 1(c), where all the sharp peaks and troughs are now represented without loss.

[Figure 1 is about here]

4.2 Example 2

This example demonstrates the movement of local orthogonality.

Consider the signal

$$S(i) = \sin(round\,(1 + i/1000) * 1000 * i * \pi / 32768) \tag{9}$$

where $i=1,2,\ldots,8200$.

The frequency of the signal $S(i)$ in (9) is constant in the intervals [0, 500), [500, 1500), [1500, 2500), [2500, 3500), [3500, 4500), [4500, 5500), 5500, 6500), [6500, 7500), and [7500, 8200]. If this function is transformed to the time-frequency domain, it will be a constant piece-wise function, and the nodes are at 500, 1500, 2500, 3500, 4500, 5500, 6500, and 7500. A wavelet decomposition of the signal in equation (9) is shown in Figure 2. Some of the orthogonalities can be recognized by inspection, for example, in the interval [6500,7500) in $j = -2$, there are 6 orthogonality locations, in the interval [2500, 3500) in $j = -3$, there are 3 orthogonality locations, and the interval [500, 1500) $j = -4$, there are 2 orthogonality locations. However, most of the local orthogonalities can only be detected by an algorithm.

[Figure 2 is about here]

Consider just the frequency components where $j = -3$, since some of the local orthogonalities in this frequency component can be clearly seen by inspection.

Selecting the phase shift values in equation (6) as $P_m = m \cdot 2^{-6}$ ($m = 0,1,\ldots,7$), a location-phase section of the frequency component $j = -3$ can be obtained using the formulation in matrix (7). In order to see the movement of the local orthogonalities corresponding to the phase shift, the frequency components have been put into one common coordinate system. In Figure 3, the frequency component corresponding to the phase shift parameter P_7 appears to be just in the right place, and those corresponding to $P_6, P_5, \ldots, P_0$ are shifted upward for 5,10, …, 35 units. In respect of each increase of the phase shift value, the local orthogonalities in the interval (2500, 3500) are moved a certain length towards the right.

[Figure 3 is about here]

Using the local orthogonality trajectory search strategy described in section 3, the local orthogonality

trajectories for the signal in equation (9) are shown in Figure 4, where the vertical axis represents the locations of the arrival points, and the horizontal axis shows the starting locations of the local orthogonalities.

[Figure 4 is about here]

The vertical axis shows the locations of the arrival points. The arrival points are also mapped to the horizontal axis, where the local orthogonalities cross the dotted line, therefore the horizontal axis shows both the departure point and the arrival points. For a single side arrival point, the other end of the line segment is a departure point, and for a double side arrival point, the two ends of the line segment are all departure points. Figure 4 shows that as the phase shifts, the orthogonalities move to the right in the intervals (700, 1500), (2500, 3500), (3500, 4500), (4500, 5500), and (5500, 7500), and move towards the left in the intervals (500, 700), (1500, 2500) and (7500, 8200). Except for k=6500, all of the other nodes of the piecewise-constant function are either departure points or arrival points, or both. The departure points are k= 700 and 2500, and the arrival points are k=500, 1500 and 7500. The points at k=3500, 4500, 5500 are both departure points and arrival points. Now 7 out of 8 discontinued points in the time-frequency domain have been detected. There are two mistakes, that at k=700 should not be judged as a discontinuous point, and the point k=6500 should have been detected. The reasons for these mistakes are that the frequency in the interval (0, 1500) is too low, and in (5500, 8200) it is too high to be analyzed in the frequency component $j=-3$, and should be analyzed in the frequency component $j=-4$ and $j=-2$, respectively. Another possibility for the failed detection is that the signal happens to be smoothly continuous in the time-space domain at k=6500, however, the length of the moving step corresponding the each phase shift in the interval (5500, 6500) and (6500, 7500) will be different.

4.3 Example 3

This example involves a monotonically continuous function in the frequency-time domain. The signal is described as

$$S(i) = \sin(i^2 \cdot \pi / 65536) \tag{10}$$

where $i = 1,2,...,8200$.

The wavelet decomposition of the given signal is shown in figure 5.

[Figure 5 is about here]

The movement of the local orthogonalities was investigated at the frequency component j=-3, and the location-phase section is shown in Figure 6.

[Figure 6 is about here]

Figure 7 shows the search results for the local orthogonality trajectories, which are very different from example 2 because the function in equation (10) is a monotonically continuous function in the frequency-time domain. Here the departure points and the arrival points are mostly double sided. Between a departure point and an arrival point of the movement of the local orthogonality, the length of the step corresponding to

each phase shift is decreased or increased untill the movement stops or oscillates at a certain location. This movement can reveal the trend of the frequency variation of a signal.

5. Application to a Permanent Magnet Synchronous Drive System

The phase shift wavelet decomposition method will be used to analyze the rotational speed of a 3-phase, 2-pole, 70V brushless permanent magnet drive system, sampled at interval of 2.5ms. A fuzzy control strategy has been designed to regulate the phase of the motor current so that the motor velocity can be maintained at a given value when the load changes. Figure 8 (a) shows the motor velocity when the current is switched on, off, and on again at t=0.5, t=2.5 and t=4.5, where the load increases, decreases, and increases again, respectively.

Figure 8 (b) shows the corresponding current amplitude based on a control strategy which uses fuzzy logic. The control strategy is very effective since the velocity is very stable even when the load is changing. However, there are too many high frequeny ripples in the current. These may cause additional acoustic noise, electro-magnetic interference, power loss, wear , and other undesirable effects.

[Figure 8 is about here]

An improved control strategy was therefore introduced based on an adaptive fuzzy method. Both the velocity and the current using the new control strategies are shown in Figure 9(a) and (b) with the same load changes as in Figure 8.

Comparing Figure 8(b) to Figure 9(b) shows that much of the high frequency ripples have been removed from the motor current.

[Figure 9 is about here]

The phase shift wavelet decomposition can be used as a tool to analyze the difference between the motor current regulated using the fuzzy controller and the adaptive fuzzy controller. The complete wavelet representation of the signals in Figure 8 (b) and Figure 9(b), are shown in Figure 10 and Figure 11, respectively.

[Figure 10 is about here]

[Figure 11 is about here]

Inspection of the two Figures shows that the major difference between Figures 10 and 11 is in the frequency components where j=-1, j=-2, and j=-3. Comparing Figure 10 and 11, the difference between the two current signals is much clearer than shown in 8(b) and 9(b), especially in the three high frequency bands, and the improvements made by the adaptive fuzzy method can be identified in each frequency component at each time location. It is easy to demonstrate that Figure 10 and 11 are also clearer that using a normal wavelet decomposition.

The local orthogonality search strategy can also be used to make a more detailed analysis. This can reveal the energies at any time location without any loss caused by local orthogonality, and the relationship between a frequency component at a location and in the neighbourhood of the location, such as continuity and smoothness.

The search results for the movement of the local orthogonalities, for instance, at j=-3, are shown in Figures 12 and 13, where a threshold of 8% of the maximum value in the frequency component has been adopted. It is very interesting to note that there exhibit two small disturbances at t=1.09 and t=1.94, where are judged as departure and arrival points.

[Figure 12 is about here]

[Figure 13 is about here]

In Figure 12, there are 13 arrival locations and the movement intervals almost cover all of the time interval [0,5]. In Figure 13, there are only 7 arrival locations and the movement intervals only cover about 46% of the time interval [0,5]. This shows that many high frequency ripples in the current have been removed by the new control strategy.

6. Conclusions

Signals can be approximated by using a wavelet expansion so that the wavelet representation can be regarded as a model of the signal and can subsequently be used for analysis of the signal. However, in a wavelet decomposition some information can be lost due to local orthogonality. Although this may not affect the approximation results it can affect the frequency analysis at each time location.

To overcome this deficiency wavelet decompositions with variable phase shift parameters were introduced in this study. For each phase shift parameter, there is a different wavelet decomposition, therefore, the same frequency component corresponding to wavelet decompositions with different phase shift parameters are also different, and the locations of the local orthogonality are shifted. A new representation of frequency components has been formulated by synthesizing all the frequency components in the same frequency band in the wavelet decomposition with different phase shift parameters. This is important in wavelet analysis, and can be helpful in searching for a better wavelet representation. One of the most important features of wavelet decompositions is that these provide a time-frequency description, and the phase shift method can make this charactistic more meaningful.

Based on the phase shift wavelet decomposition, the movement of the locations of local orthogonalities corresponding to phase shifts are detected, and are shown to reveal many features of the given signal, such as continuity, smoothness and trends. This could be very important in signal analysis, for example, it has potential in fault detection and diagnosis. For different kinds of fault in a system, the local orthogonal trajectories will be different, and each of these can be regarded as a pattern. By combining these ideas with an artificial intelligence technique, it should be possible to develop an effective fault detection and diagnosis

system.

Acknowledgement

JL and SAB gratefully acknowledge that part of this research was supported by the UK Engineering and Physical Science Research Council.

REFERENCES

1. I. Daubechies. Orthonormal bases of compactly supported wavelets. Communications on Pure & Applied Math. Vol.41, 1988, pp. 909-996.
2. I. Daubechies. The wavelet transformation, time-frequency localization and signal analysis. IEEE Trans. On Information Theory, Vol. 36, 1990, pp. 961-1005.
3. C. K. Chui. An introduction to wavelets, Academic Press, Boston, 1992.
4. A. Judisky, H. Hjalmarsson, A. Benveniste, B. Delyon, L. Ljung, J. Sjoberg and Q. Zhang. Nonlinear black-box models in system identification: Mathematical foundations. Automatica, Vol.31, No. 12, 1995, pp. 1725-1750.
5. Y. C. Pati and P. S. Krishnaprasad. Analysis and Synthesis of Feed-forward Neural Networks Using Discrete Affine Wavelet Transformations. IEEE Trans. on Neral Networks, Vol. 4, 1993, pp. 73-85
6. Q. Zhang and A. Benveniste, Wavelet networks. IEEE Tranc. NN, Vol. 3, No. 6, Nov. 1992, pp.889-898.
7. Q. Zhang. Using Wavelet Network in Nonparametric Estimation. IEEE Trans. Neural Networks, Vol. 8, No. 2, 1997.
8. H. S. Stone. Progressive Wavelet Correlation Using Fourier Methods. IEEE Trans. on Signal Processing, Vol. 47, No. 1, 1999, pp. 97-107.
9. Y. Meyer. Ondelettes. Fonctions Splines et Analyses Graduees. Lectures given at the University of Torino, 1986, Italy.
10. S. Mallat. Multiresolution Approximation and Wavelets. Trans. Amer. Math. Soc.,315, 1989, pp. 69-88.
11. D. Coca and S. A. Billings. Continuous-Time System Identification for Linear and nonlinear Systems Using Wavelet Decompositions. International Journal of Bifurcation and Chaos, Vol. 7, No. 1, 1997, pp. 87-96.
12. R. D. Nowak and R. G. Baraniuk. Wavelet-Based Transformations for Nonlinear Signal Processing. IEEE Trans. on Signal Processing, Vol. 47, No. 7, 1999, pp. 1852-1865.
13. T. Xia and Q. Jiang. Optimal Multifilter Banks: Design, Related Symmetric Extension Transform, and Application to Image Compression. IEEE Trans. on Signal Processing, Vol. 47, No. 7, 1999, pp. 1878-1889.
14. G. Evangelista and S. Cavaliere. Frequency-Warped Filter Banks and Wavelet Transforms: A Discrete-Time Approach via Laguerre Expansion. IEEE Trans. on Signal Processing, Vol. 46, No. 10, 1998, pp. 2638-2650.
15. J. T. Miller and C.-C. Li. Adaptive Multiwavelet Initialization. IEEE Trans. on Signal Processing, Vol. 46, No. 12, 1998, pp. 3282-3291.
16. Q. Jiang. On the Design of Multifilter Banks and Orthonormal Multiwavelet Bases. IEEE Trans. on Signal Processing, Vol. 46, No. 12, 1998, pp. 3292-3303.

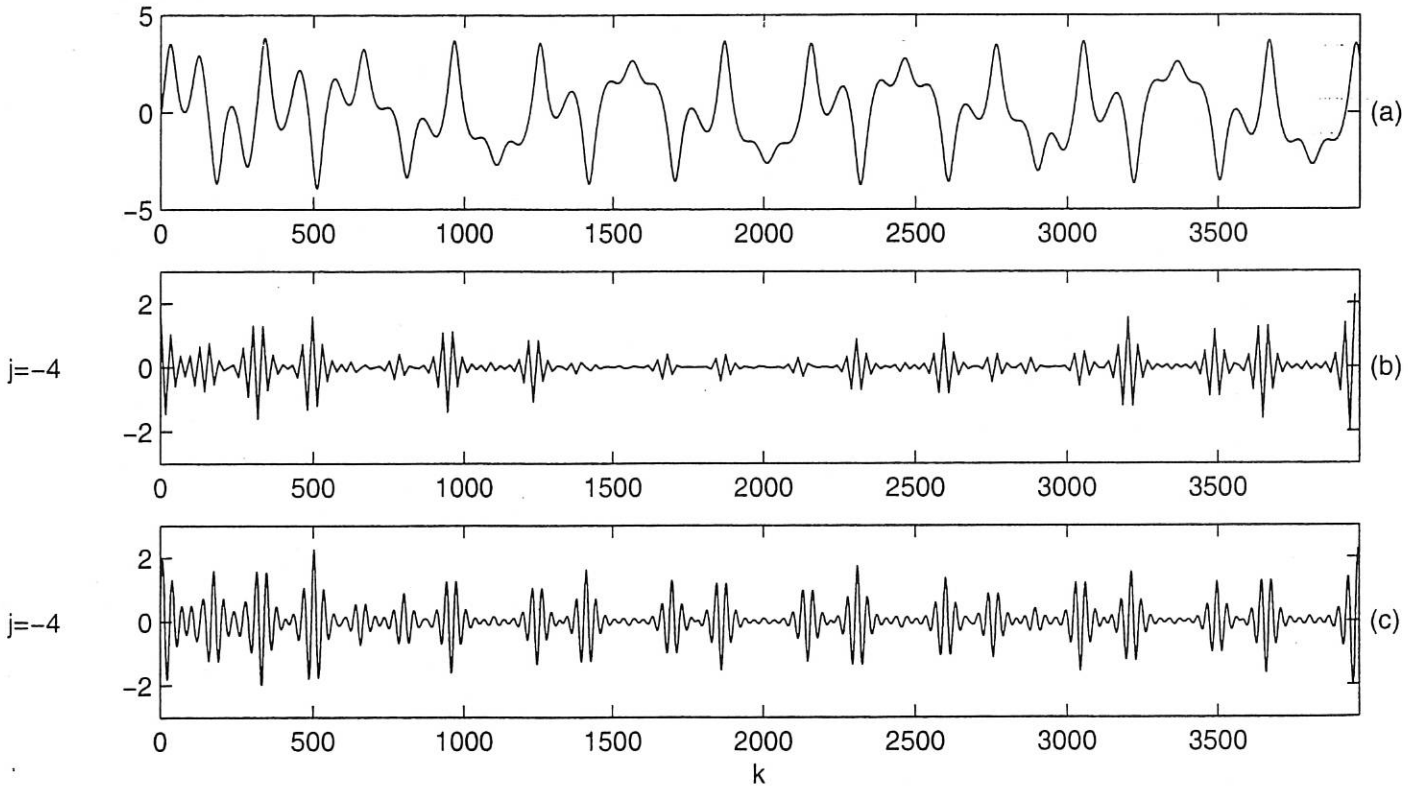

Figure 1 (a) Data generated from the Duffing equation

(b) The normal wavelet frequency component representation at j=−4

(c) The phase shift wavelet frequency component representation at j=−4

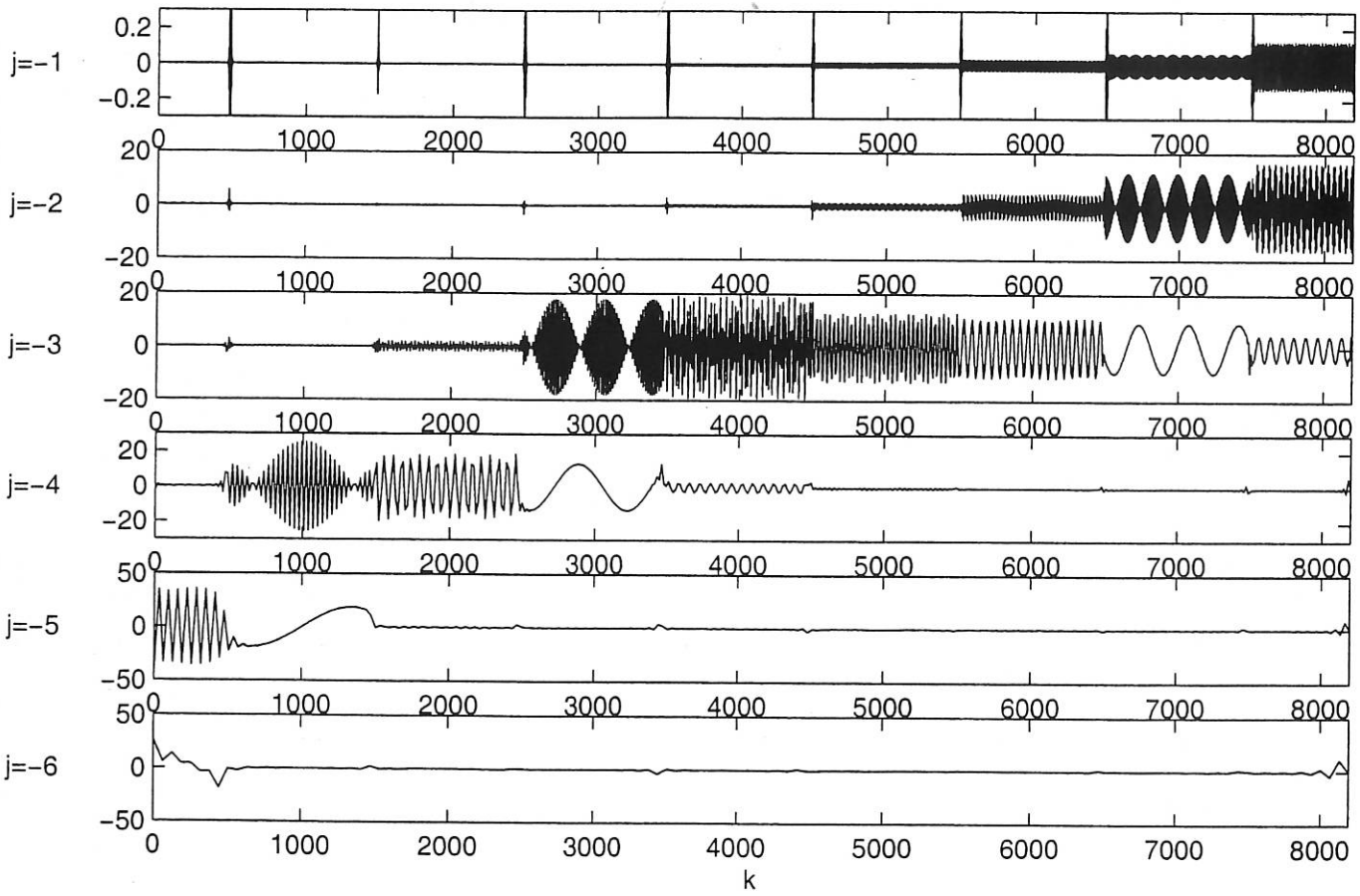

Figure 2 A wavelet decomposition of the signal in example 2 from j=−1 to j=−6.

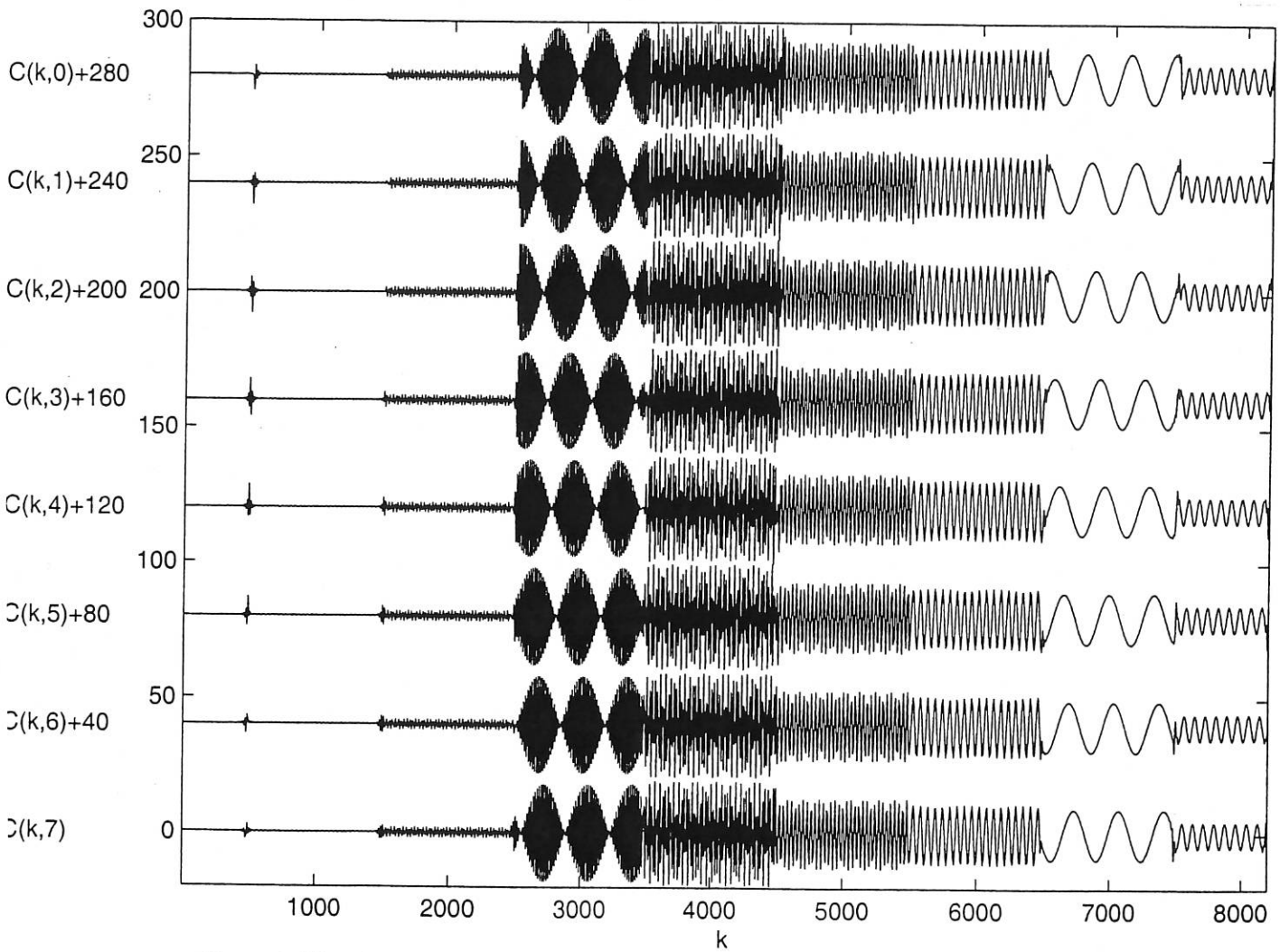

Figure 3 The phase-time section of the frequency component at j=-3.

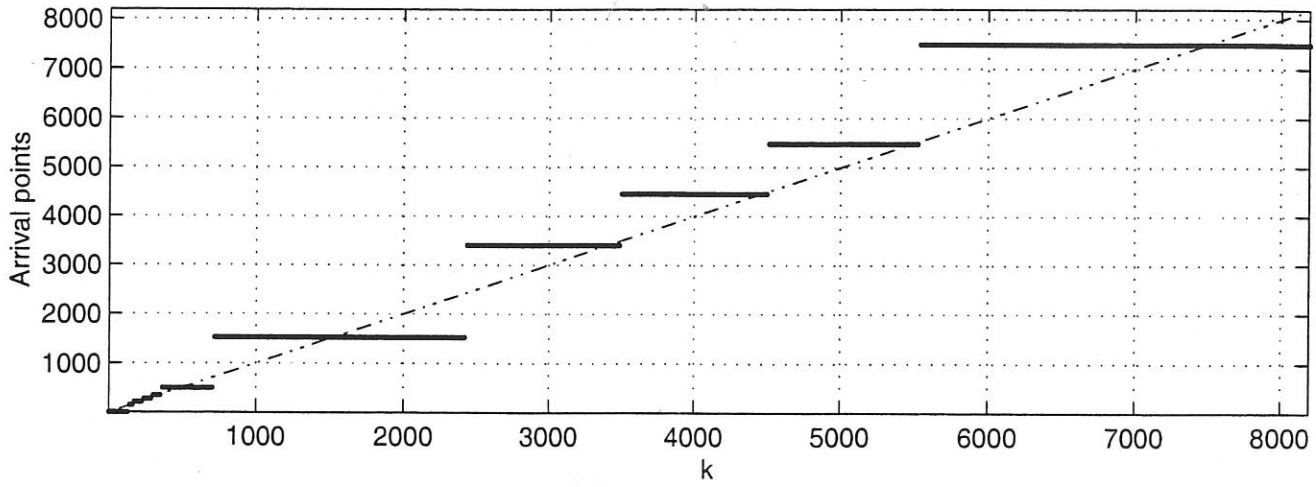

Figure 4 The results of the search for the movement of local orthogonalities.

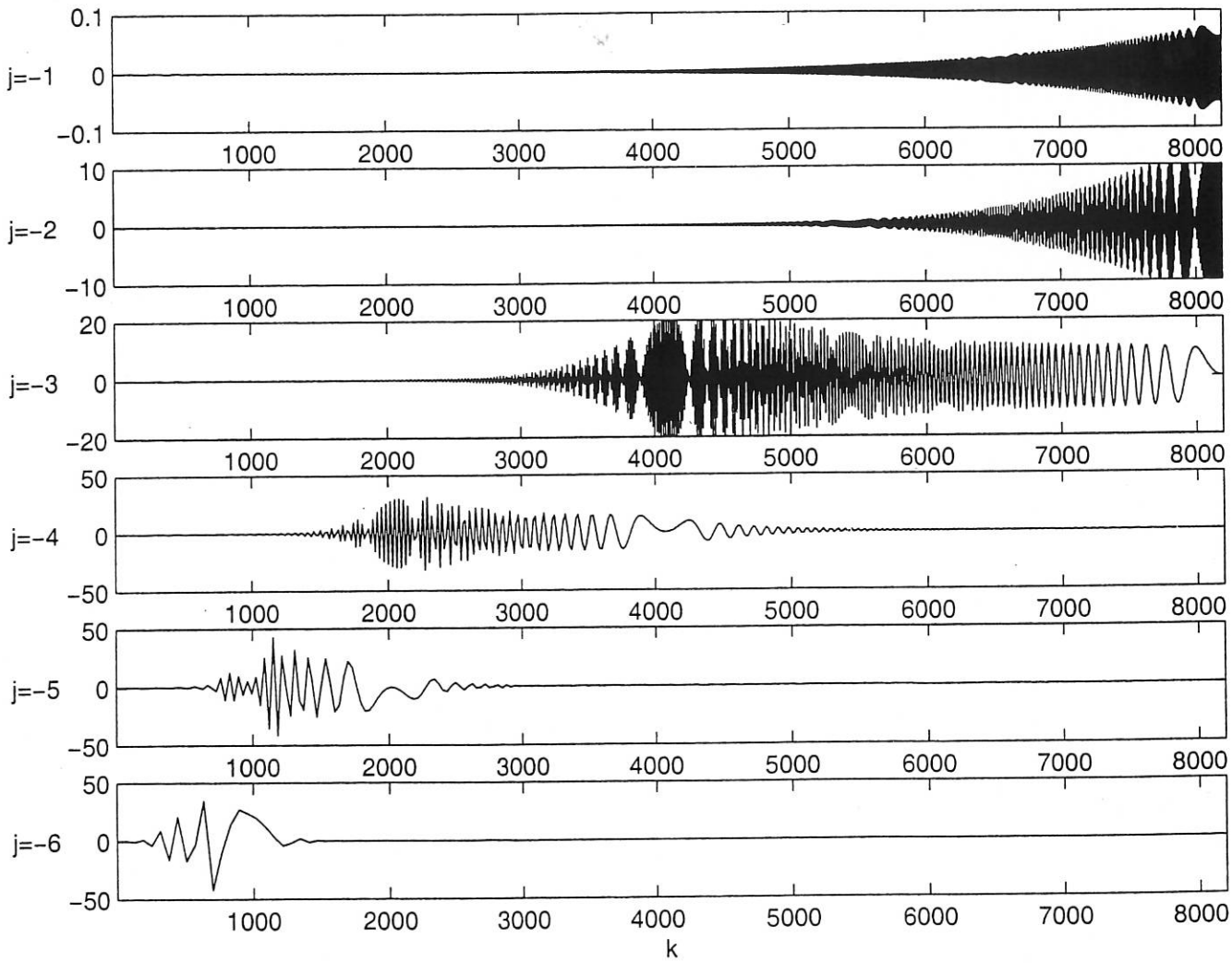

Figure 5 A wavelet decomposition of the signal in example 3 from j=−1 to j=−6.

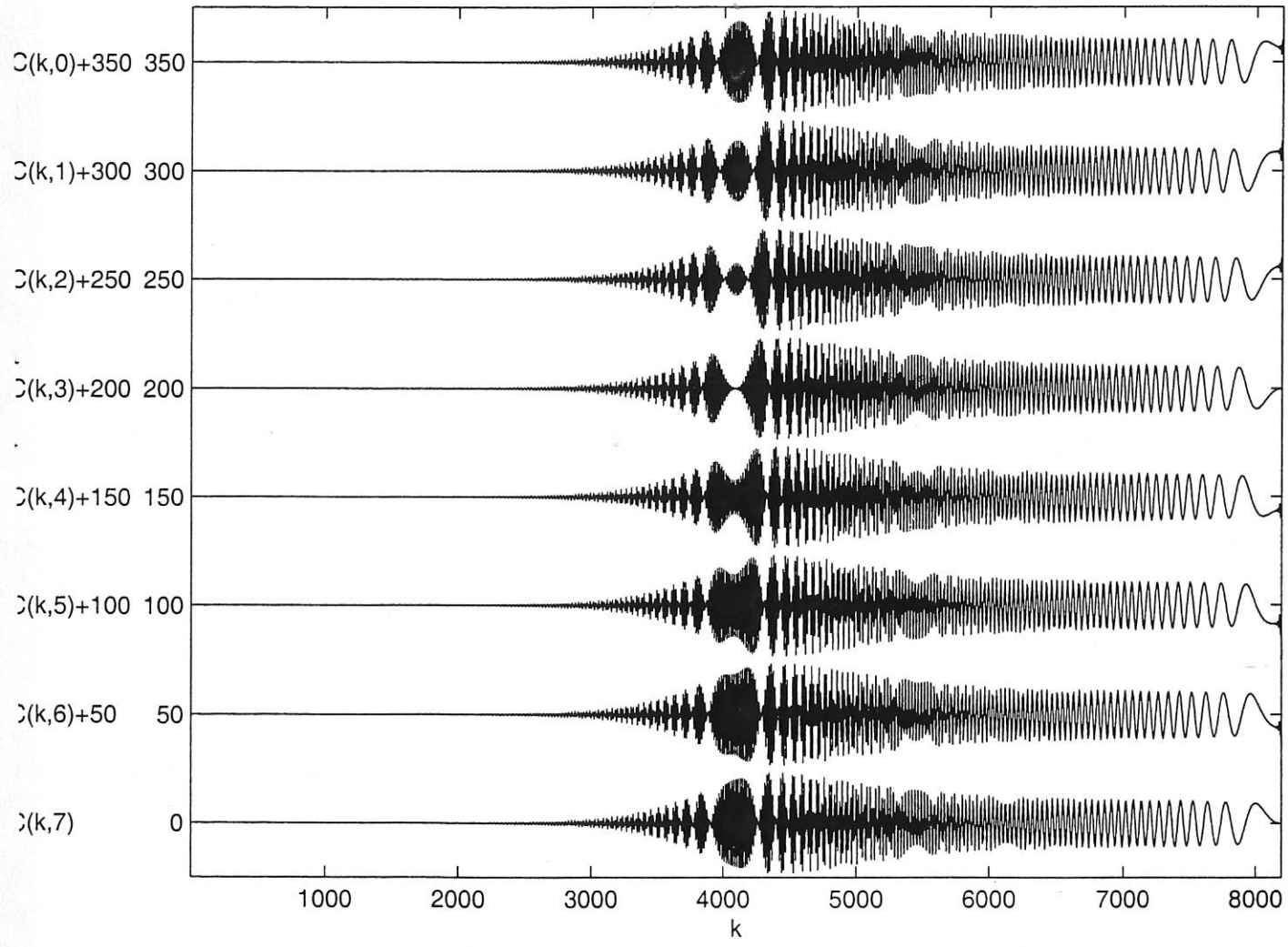

Figure 6 The phase-time section of the frequency components at j=-3.

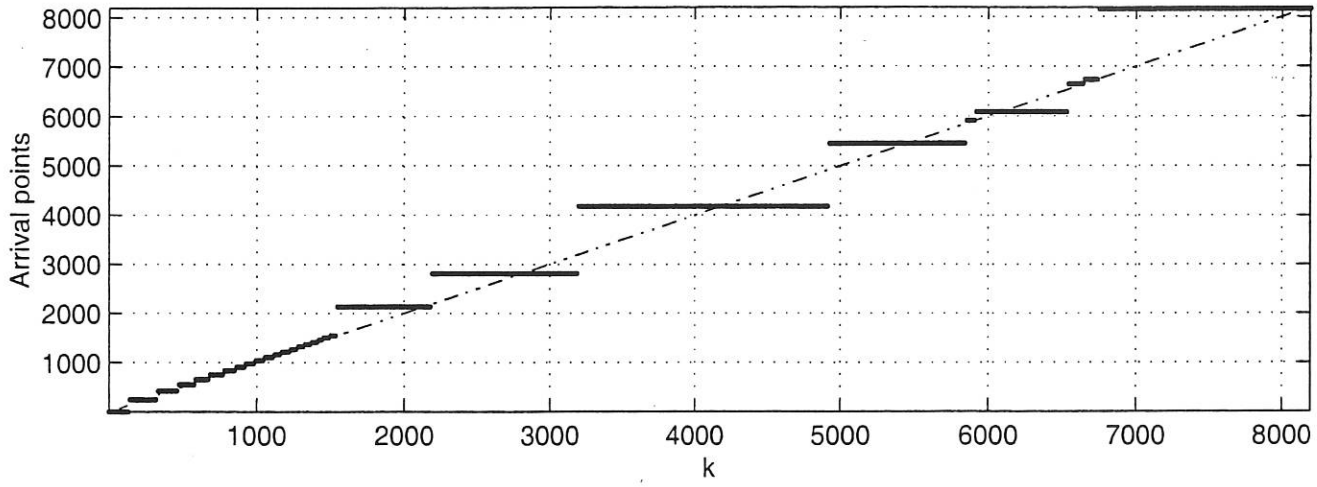

Figure 7 The results of the search for the movement of the local orthogonalities.

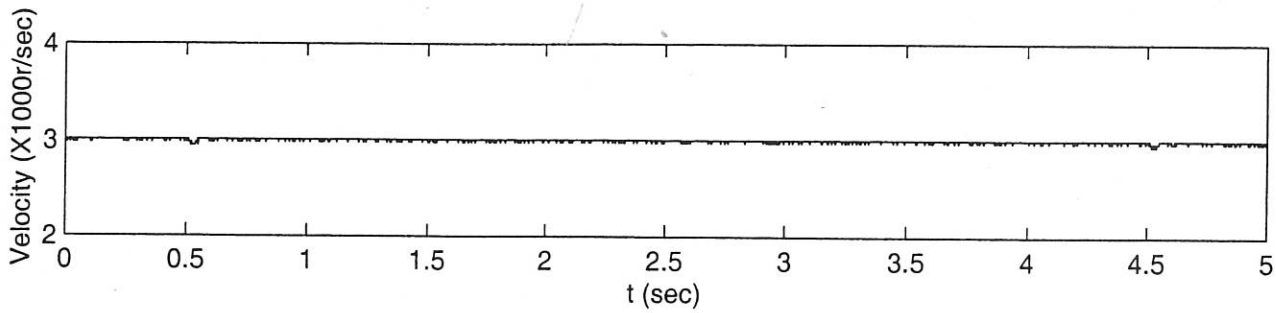

Figure 8(a) The rotational speed of motor

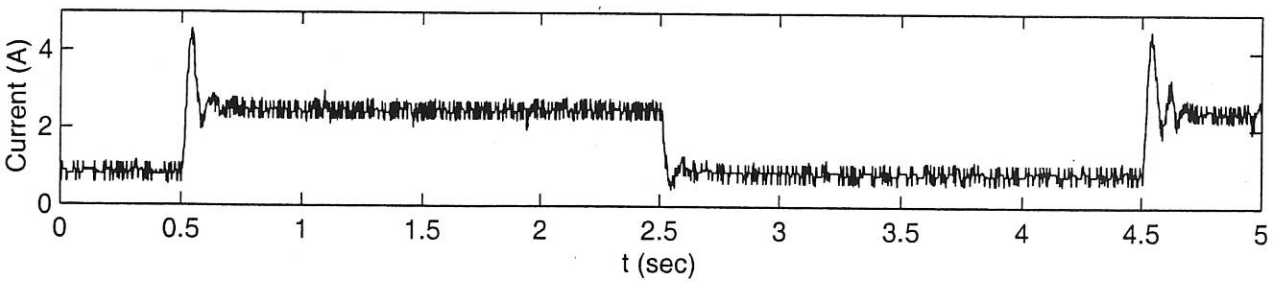

Figure 8(b) The current ampltude controlled by fuzzy logic

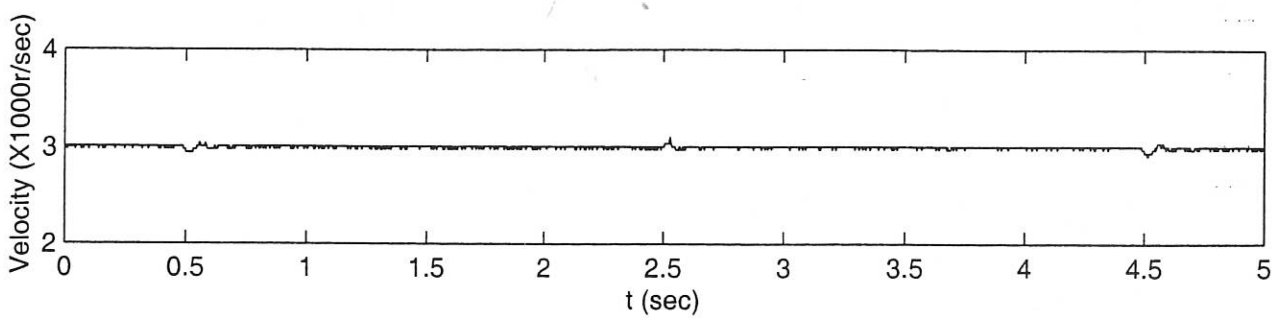

Figure 9(a) The rotational speed of motor

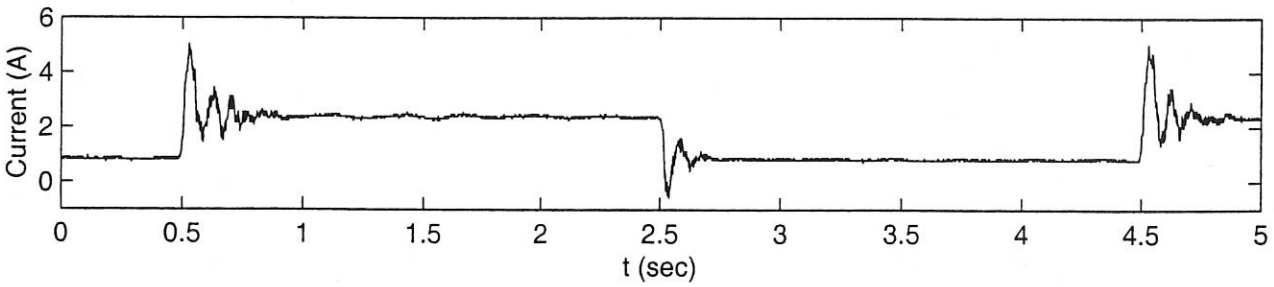

Figure 9(b) The current amplitude controlled by an adaptive fuzzy method

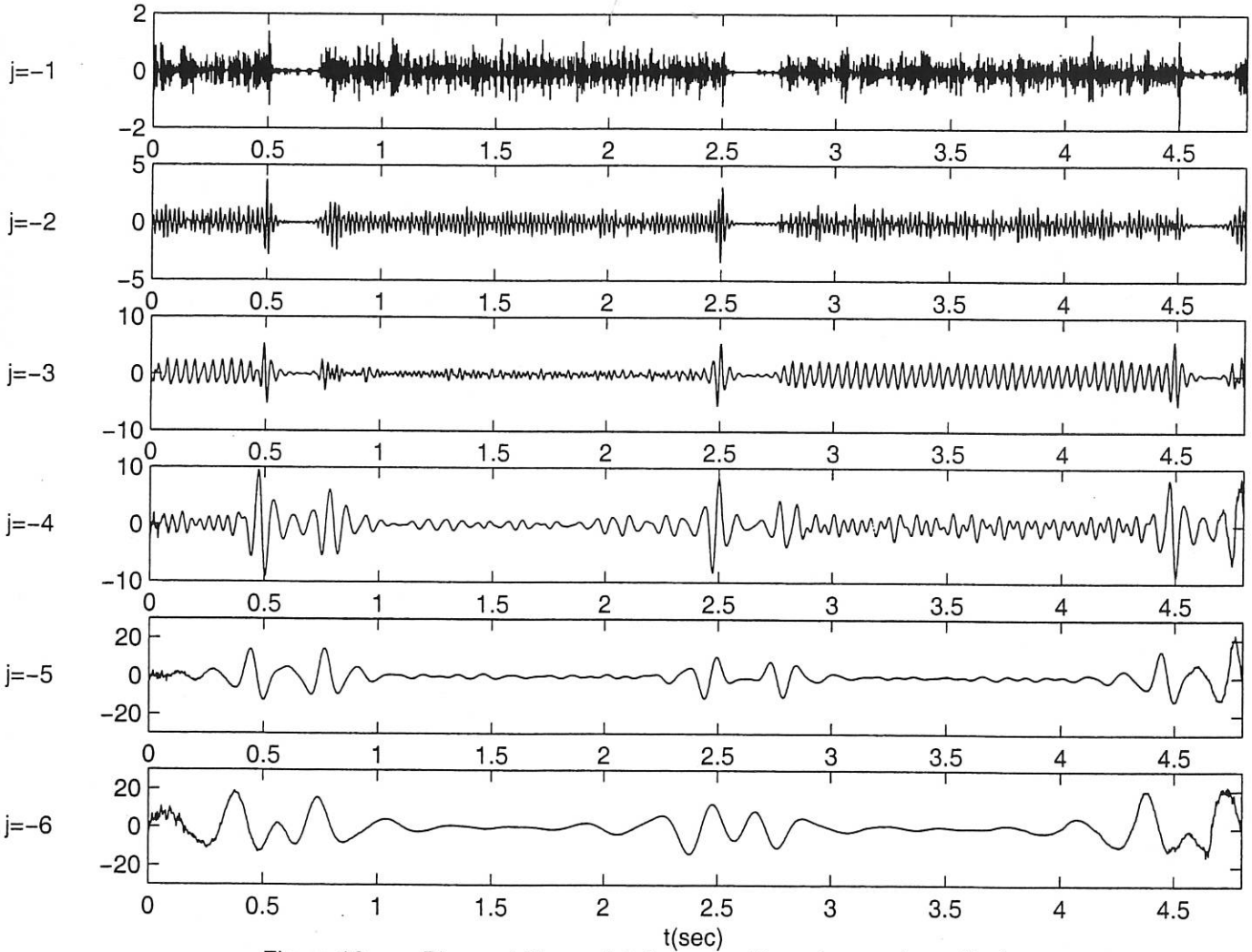

Figure 10 Phase shift wavelet decomposition of current amplitude controlled by fuzzy logic shown in Figure 8(b)

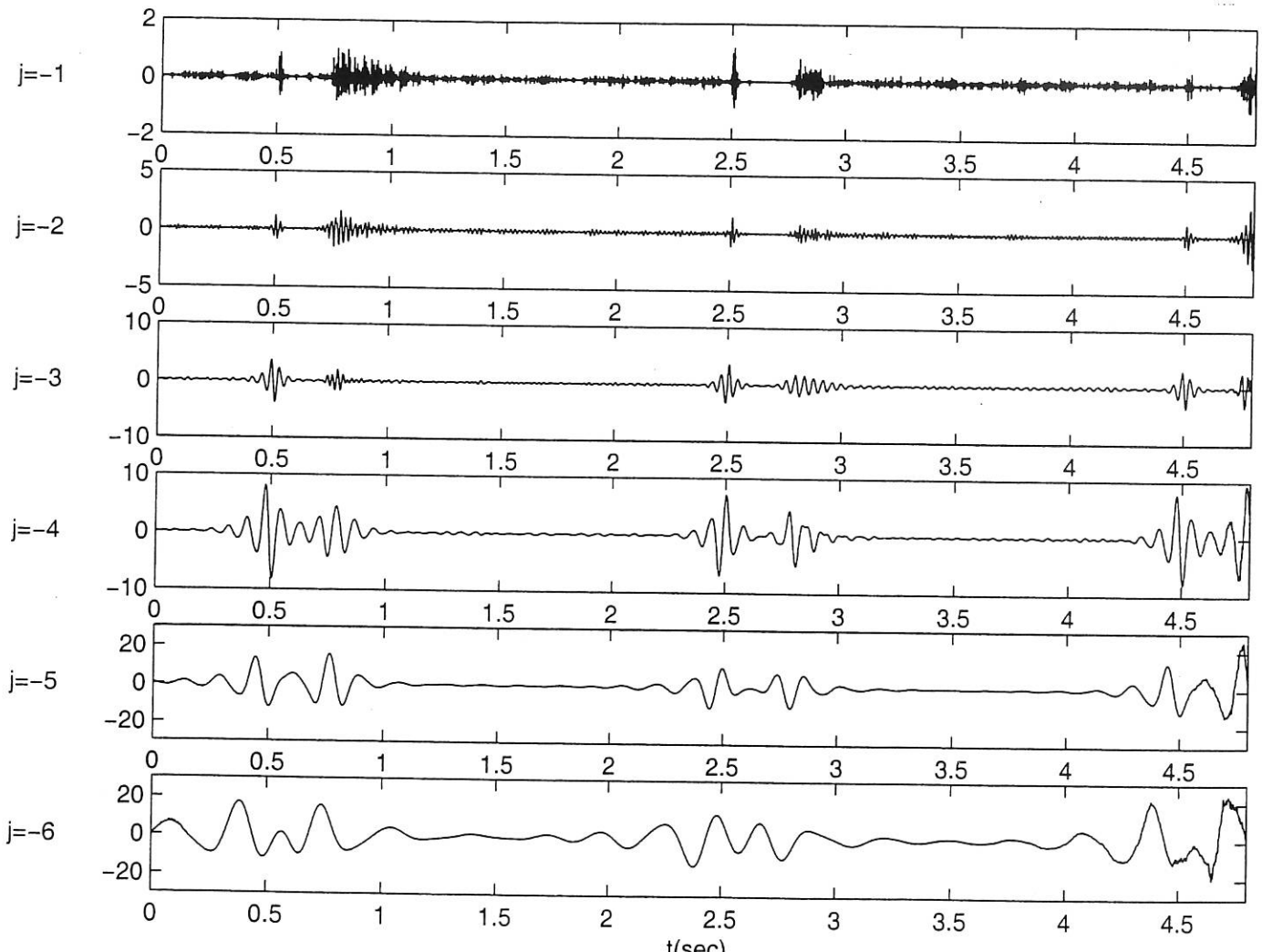

Figure 11 Phase shift wavelet decomposition of current amplitude controlled by an adaptive fuzzy method shown in figure 9(b)

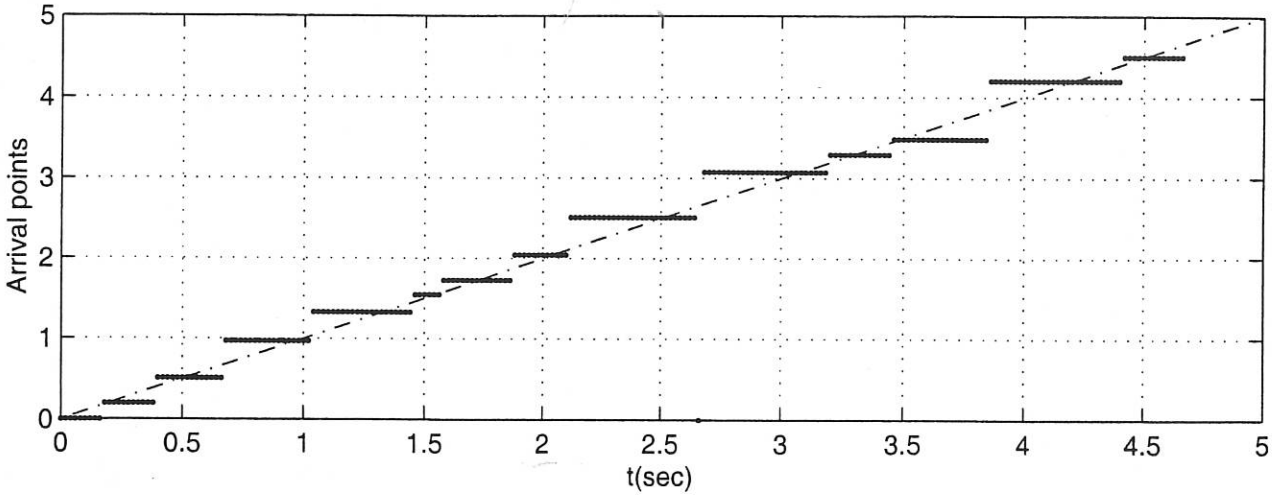

Figure 12 The search result of the local orthogonality movement for the signal in Figure 8(b) with threshold 0.08

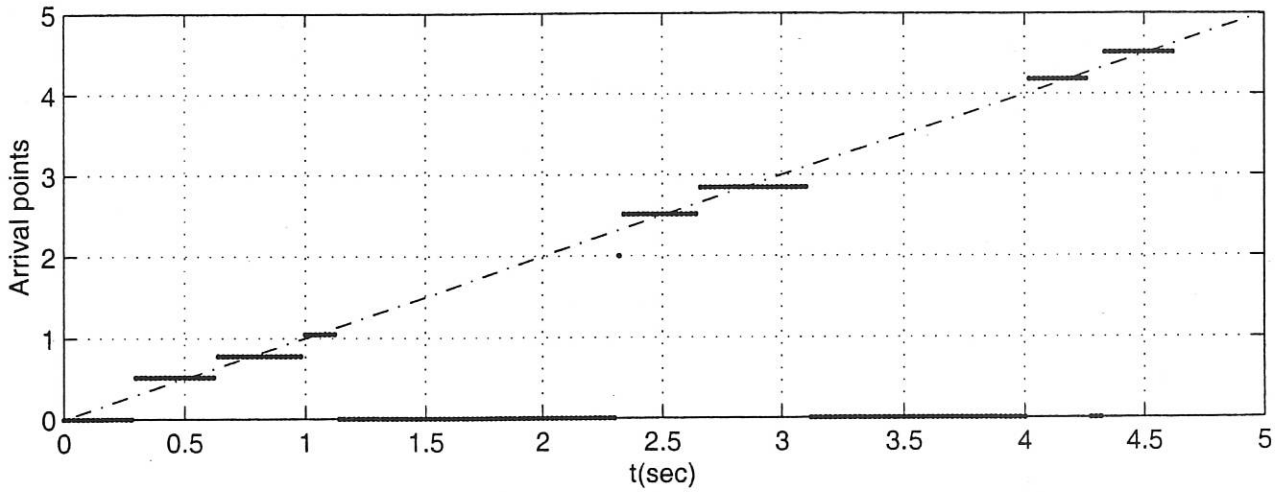

Figure 13 The results of the search for the movement of the local orthogonalities for the improved signal in Figure 9(b) with threshold 0.08